Predictor–Corrector Quasi-Static Method Applied to Nonoverlapping Local/Global Iterations with 2-D/1-D Fusion Transport Kernel and p-CMFD Wrapper for Transient Reactor Analysis

Bumhee Cho and Nam Zin Cho*
Korea Advanced Institute of Science and Technology (KAIST)
291 Daehak-ro, Yuseong-gu, Daejeon, Korea 34141
**Corresponding author: nzcho@kaist.ac.kr*

1. Introduction

CRX-2K [1] is a transport code which has a transient capability for the whole-core transport calculation. CRX-2K adopts the nonoverlapping local/global (NLG) iterative method with the 2-D/1-D fusion transport kernel and the global p-CMFD wrapper. The parallelization of the NLG iteration has been recently implemented in CRX-2K and several numerical results are reported in a companion paper [2]. However, the direct time discretization leads to a fine time step size to acquire an accurate transient solution, and the step size involved in the transport transient calculations is millisecond-order [1, 3, 4]. Therefore, the transient calculations need much longer computing time than the steady-state calculation.

To increase the time step size, Predictor-Corrector Quasi-Static (PCQS) method [5] can be one option to apply to the NLG iteration. The PCQS method is a linear algorithm, so the shape function does not need to be updated more than once at a specific time step like a conventional quasi-static (QS) family such as Improved Quasi-Static (IQS) method [6]. Moreover, the shape function in the PCQS method directly comes from the direct transport calculation (with a large time step), so one can easily implement the PCQS method in an existing transient transport code.

Any QS method needs to solve the amplitude function in the form of the point kinetics (PK) equations, and accurate PK parameters can be obtained by the transport steady-state adjoint angular flux as a weighting function. However, it is computationally costly to solve the adjoint transport equation.

In this study, the steady-state p-CMFD adjoint flux is used as the weighting function to obtain PK parameters instead of the computationally expensive transport adjoint angular flux. Several numerical problems are investigated to see the capability of the PCQS method applied to the NLG iteration.

2. Adjoint p-CMFD Equation

To avoid the expensive calculation to obtain the adjoint angular fluxes, the p-CMFD adjoint scalar flux will be used to obtain the PK parameters.

2.1 Steady-State p-CMFD Equation

The steady-state transport equation is given as follows:

$$\vec{\Omega}\cdot\nabla\psi_g+\sigma_{t,g}\psi_g=\frac{1}{4\pi}\left[\frac{1}{k_{eff}}\chi_g\sum_{g'}\nu\sigma_{f,g'}\phi_{g'}+\sum_{g'}\sigma_{s0,g'\to g}\phi_{g'}\right], \tag{2.1}$$

where all notations are standard in reactor physics.

To formulate p-CMFD equation, Eq. (2.1) is homogenized, condensed, and integrated in a coarse group G and a coarse mesh I:

$$\sum_{u=x,y,z}\sum_{s=0,1}\frac{J^{+,I}_{G,u,s}-J^{-,I}_{G,u,s}}{H^I_u}+\sigma^I_{r,G}\phi^I_G=\frac{\chi^I_G}{k_{eff}}\sum_{G'}\nu\sigma^I_{f,G}\phi^I_{G'}+\sum_{G'\neq G}\sigma^I_{s0,G'\to G}\phi^I_{G'}, \tag{2.2}$$

where all quantities are defined in elsewhere [1].

In the p-CMFD methodology, the transport partial currents are preserved by the following relations [7, 8]:

$$J^{+,I}_{G,u,s}=\frac{-\tilde{D}_{G,u,s}(\phi^{I^{s^*}}_G-\phi^I_G)+2\hat{D}^+_{G,u,s}\phi^I_G}{2}, \tag{2.3}$$

$$J^{-,I}_{G,u,s}=\frac{\tilde{D}_{G,u,s}(\phi^{I^{s^*}}_G-\phi^I_G)+2\hat{D}^-_{G,u,s}\phi^{I^{is^*}}_G}{2}. \tag{2.4}$$

where I^{s^*} is the nearest coarse mesh index to the surface s of the coarse mesh I.

By substituting Eqs. (2.3) and (2.4) into Eq. (2.2), the equation is formulated only by the scalar flux, and it can be expressed in the following matrix form:

$$\mathrm{T}_0\phi_0=\frac{1}{k_{eff}}F_0\phi_0, \tag{2.5}$$

where
F_0 is the fission operator in steady-state,
T_0 is the transport operator in steady-state except the fission operator.

2.2 Adjoint p-CMFD Equation

The corresponding adjoint equation is obtained by simply transposing the operators in Eq. (2.5) [6]:

$$\mathrm{T}_0^*\phi_0^* = \frac{1}{k_{eff}^*}F_0^*\phi_0^*. \tag{2.6}$$

Note that k_{eff}^* is same with k_{eff}. The solution of Eq. (2.6) can be obtained with little modification of the existing solver for Eq. (2.5). The adjoint scalar flux obtained by the low-order form of the transport equation (in this study, Eq. (2.6)) is obviously different from the scalar flux integrated by the transport adjoint angular flux:

$$\phi_0^* \neq \int_I\int_\Omega \psi_0^* d\Omega dV. \tag{2.7}$$

Though they are different as shown in the literature [9], this fact is not a critical issue in reactor applications. The main purpose of the adjoint solution is to evaluate "best" PK parameters, and little-degraded adjoint flux by the p-CMFD equation would have negligible impact on the evaluation. Note that the PK parameters can be obtained by arbitrary weighting functions, and the adjoint solution is one of them (but best).

3. PCQS Method in NLG Iteration

Instead of the adjoint angular flux by the transport equation, the adjoint scalar flux by the p-CMFD equation will be used as the weighting function to evaluate the PK parameters.

3.1 PK Equations

To derive the PK equations, let us consider the following time-dependent transport equation:

$$\frac{1}{v}\frac{\partial\psi}{\partial t} = \frac{1}{4\pi}F^p\psi - M\psi + \frac{1}{4\pi}\sum_d \chi_d(E)\lambda_d C_d(t), \tag{3.1}$$

$$\chi_d(E)\frac{\partial C_d}{\partial t} = -\chi_d(E)\lambda_d C_d + F_d\psi, \tag{3.2}$$

where

ψ is the angular flux as a function of $\vec{r}$, E, $\vec{\Omega}$, and t,

$$F^p\psi = \frac{(1-\beta)}{k_{eff}}\chi_p(E)\int_E\int_\Omega \nu\sigma_f(E)\psi\, d\Omega dE,$$

$$M\psi = \Omega\cdot\nabla\psi + \sigma_t\psi - \frac{1}{4\pi}\int_{E'}\int_\Omega \sigma_{s0}(E'\to E)\psi\, d\Omega dE',$$

$$F_d\psi = \frac{\beta_d}{k_{eff}}\chi_d(E)\int_E\int_\Omega \nu\sigma_f(E)\psi\, d\Omega dE,$$

and other notations are standard in reactor physics.

The main idea of any kind of QS methods is the factorization of angular (or scalar) flux into "amplitude" and "shape" functions [10, 11]. Following the strategy, the angular flux in Eq. (3.1) is factorized as follows:

$$\psi(\vec{r},\vec{\Omega},t) = T(t)\varphi(\vec{r},\vec{\Omega},t). \tag{3.3}$$

Note that this factorization holds for a slowing varying shape function in time. In addition, the following normalization condition is forced in time:

$$\left\langle \phi_0^*, \frac{1}{v}\varphi \right\rangle := C \equiv \left\langle \phi_0^*, \frac{1}{v}\psi_0 \right\rangle. \tag{3.4}$$

By substituting Eq.(3.3) into Eqs. (3.1) and (3.2), multiplying the adjoint "scalar" flux obtained by the p-CMFD equation, and integrating over all variables, then the following PK equations are obtained:

$$\frac{\partial T(t)}{\partial t} = \frac{\rho(t)-\beta^{eff}(t)}{\Lambda(t)}T(t) + \frac{1}{\Lambda_0}\sum_d \bar{\lambda}_d(t)c_d(t), \tag{3.5}$$

$$\frac{\partial c_d(t)}{\partial t} = -\bar{\lambda}_d(t)c_d(t) + \frac{\Lambda_0}{\Lambda(t)}\beta_d^{eff}(t)T(t), \tag{3.6}$$

where

$$\rho(t) = \frac{1}{\hat{f}(t)}\left\langle \phi_0^*, \left(\frac{1}{4\pi}F^p - M\right)\varphi \right\rangle,$$

$$\beta_d^{eff}(t) = \frac{1}{\hat{f}(t)}\left\langle \phi_0^*, \frac{1}{4\pi}F_d\psi \right\rangle,$$

$$\beta^{eff} = \sum_d \beta_d^{eff},$$

$$\Lambda(t) = \frac{1}{\hat{f}(t)}\left\langle \phi_0^*, \frac{1}{v}\varphi \right\rangle, \text{ note that } \Lambda(t)\hat{f}(t) = \Lambda_0\hat{f}_0,$$

$$\hat{f}(t) \equiv \left\langle \phi_0^*, \left(F_p\psi + \sum_d F_d\psi\right)\varphi \right\rangle.$$

Therefore, the PK equations, Eqs. (3.5) and (3.6), can be solved by any kind of ODE solver once the shape function is given. Note that the computing time to solve the PK equations is negligible compared to the NLG iteration.

3.2 Shape Function

Let us assume that a "predicted" transport solution at time step t_{n+1} (with a relatively large time step size) is given by $\tilde{\psi}(t_{n+1})$, and the solution is obtained by the transient NLG iteration with the 2-D/1-D fusion kernel and the global p-CMFD wrapper as described in the literatures [1, 2]. With the predicted solution, one can evaluate the following quantity:

$$Z \equiv \left\langle \phi_0^*, \frac{1}{v}\tilde{\psi} \right\rangle / C. \tag{3.7}$$

Then, one can find the shape function satisfying Eq. (3.4) by the following equation:

$$\varphi = \frac{1}{Z}\tilde{\psi}. \tag{3.8}$$

Therefore, the PK parameters in Eqs. (3.5) and (3.6) are evaluated using the shape function, Eq. (3.8), and then, the PK equations (3.5) and (3.6) can be solved.

3.3 PK Parameters by p-CMFD Solution

As described, the weighting function is the angle-independent p-CMFD adjoint scalar flux, so the PK parameters can be evaluated only by the solutions of the p-CMFD equations (forward and adjoint). The detailed expressions of the PK parameters are given as follows:

$$\rho = \frac{1}{\hat{f}} \sum_G \sum_I V^I \phi_{0,G}^{*,I} \times \left(\begin{array}{l} \frac{1}{k_{eff}} \chi_G^I \sum_{G'} \nu\Sigma_{f,G'}^I \phi_{G'}^I + \sum_{G'} \Sigma_{s0,G'\to G}^I \phi_{G'}^I \\ + \sum_{u=x,y,z} \sum_{s=0,1} \left[\frac{\left(\tilde{D}_{G,u,s} + \hat{D}_{G,u,s}^- \right)}{H_u^I} \phi_G^{I^{s^*}} \right] \\ - \left[\Sigma_{t,G} + \sum_{u=x,y,z} \sum_{s=0,1} \left[\frac{\left(\tilde{D}_{G,u,s} + \hat{D}_{G,u,s}^+ \right)}{H_u^I} \right] \right] \phi_G^I \end{array} \right), \tag{3.9}$$

$$\beta_d^{eff} = \frac{1}{\hat{f}} \sum_G \sum_I V^I \phi_{0,G}^{*,I} \times \left(\chi_{d,G}^I \frac{\bar{\beta}_d^I}{k_{eff}} \sum_{G'} \nu\Sigma_{f,G'} \phi_{0,G}^I \right), \tag{3.10}$$

$$\Lambda = \frac{1}{\hat{f}} \sum_G \sum_I V^I \phi_{0,G}^{*,I} \times \left(\frac{1}{v_G^I} \phi_G \right), \tag{3.11}$$

$$\hat{f} = \sum_G \sum_I V^I \phi_{0,G}^{*,I} \times \left(\frac{1}{k_{eff}} \chi_G^I \sum_{G'} \nu\Sigma_{f,G'}^I \bar{\phi}_{G'} \right). \tag{3.12}$$

The solution and homogenized quantities are given by the results of the NLG iteration. The overall flowchart of the NLG iteration with the PCQS method is shown in Fig. 1.

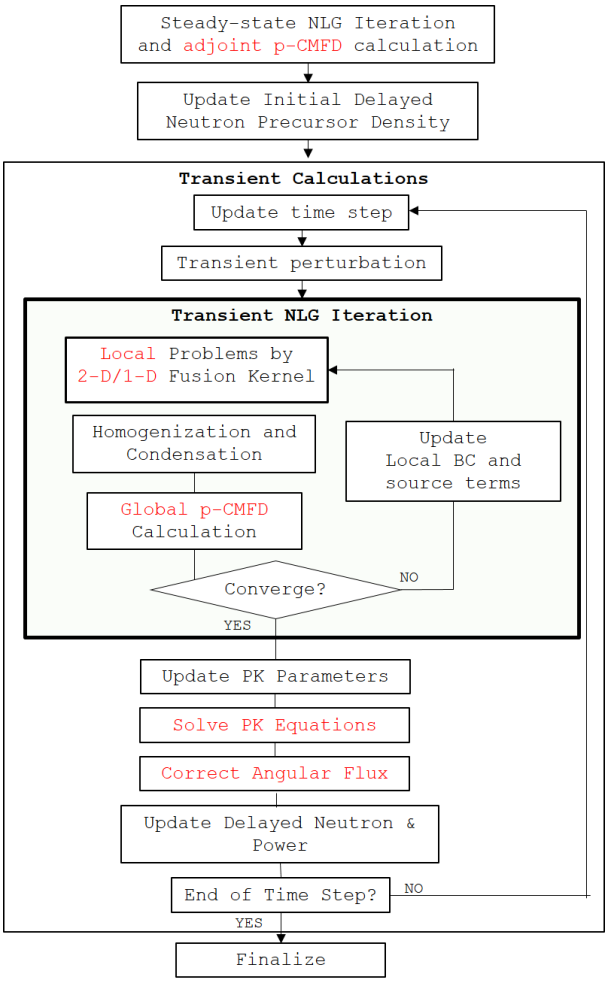

Fig. 1. Flowchart of NLG iteration with PCQS method

4. Further Means for Increasing Time-Step Size

In this study, the PCQS method has been adopted to increase the time-step size. As already mentioned, the PCQS may not work when the shape function changes significantly in time. Therefore, additional ideas are warranted to increase the time-step size.

4.1 Exponential Transformation

The exponential transformation [12] can be applicable to the time derivative term of the angular flux in the transport equation. The exponential transformation has been widely used in diffusion theory finite difference and nodal methods and successfully increased the time-step size. Moreover, more stable calculational procedure can be obtained by this method. One can derive the exponential-transformed-time-discretized transport equation by the following ansatz:

$$\psi_g(\vec{r},\vec{\Omega},t) = \tilde{\psi}_g(\vec{r},\vec{\Omega},t) e^{w_g t}. \tag{4.1}$$

Note that $\tilde{\psi}_g(\vec{r},\vec{\Omega},t)$ is a slowly varying function.

4.2 Intermediate p-CMFD Updates

As the PK equations assume the whole-core domain as a single point, inter-assembly transport effects are not reflected during a macro time step. Therefore, the PCQS method may hold only for a slowly varying shape function. To consider transport effects efficiently during the course of a macro time step, the p-CMFD equation can be used to predict the change of shape function with finer time steps than the macro time step. By this strategy, the shape function required in the PCQS method would be more precise, so the macro time-step size can be increased further.

5. Numerical Results

The numerical problems consist of two problems; 1) a two-dimensional homogeneous problem, 2) a three-dimensional heterogeneous single assembly rod ejection problem. The NLG iteration with the PCQS method has been implemented in CRX-2K, and parallelization is applied to the NLG iteration [1, 2]. Calculational conditions are set to give an accurate solution, but not shown in this paper for the sake of brevity.

All numerical calculation is carried out by the NLG iteration with the parallel computing nodes. The comparison between the NLG iteration and the p-CMFD acceleration is discussed in the literature [1, 2]. Intel Xeon X5670 @ 2.93 GHz was used for the calculations.

5.1 TWIGL 2G Problem

TWIGL 2G problem is a two-dimensional and two-group problem [13]. The cross sections and the information of delayed neutron precursors are given in the literature [1]. The geometry is shown in Fig. 2, and the transient event occurs by the linear or step jump changes of the cross sections of region 1 in time.

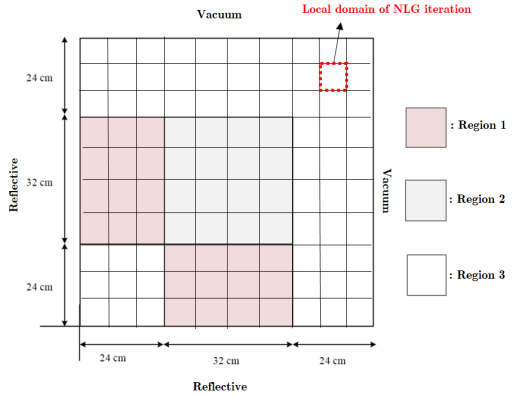

Fig. 2. Geometry (TWIGL 2G)

The results are shown in Figs. 3, 4 and Table I. The reference calculation was carried out by the NLG iteration without the PCQS method with 1 ms time step size, and the time step size should be less than 1 ms to capture the reactivity jump effect in this problem. Here and after, "DIRECT" stands for the transient NLG iteration without the PCQS method, and "PCQS" stands for the NLG iteration with the PCQS method.

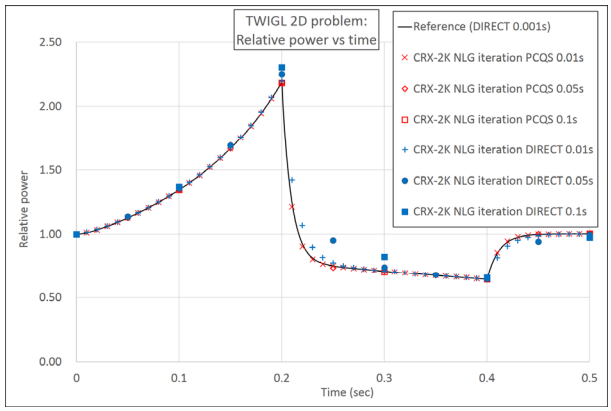

Fig. 3. Relative power vs time (TWIGL 2G)

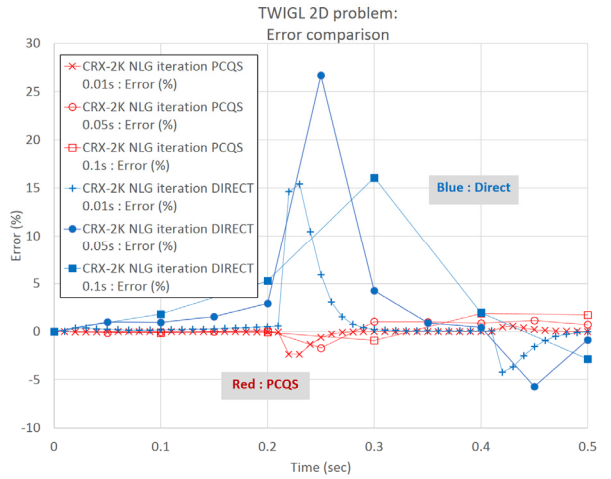

Fig. 4. Percentage error vs time (TWIGL 2G)

As shown in Fig. 3, PCQS agrees well with the reference solution even with the 0.1 sec time step size. The errors by DIRECT are large, while PCQS has quite small errors as shown in Fig. 4 and Table I. The computing time obviously takes less as the larger time step size is used both in DIRECT and PCQS as shown in Table I. With the same time step size, DIRECT takes less time than PCQS as shown in Table I, since PCQS finds the solution at a specific time step to reflect (capture) the corrected flux of the previous time step. However, a computing time comparison between DIRECT and PCQS with large time steps is meaningless, since DIRECT with large time steps causes very inaccurate solutions.

Table I: Result summary (TWIGL 2G)

Method	Time step size (sec)	Maximum error (%)	Maximum error point (sec)	Computing time (sec)
DIRECT	0.01	14.64	0.22	1554.5
	0.05	26.67	0.25	492.9
	0.1	16.09	0.3	314.2
PCQS	0.01	-2.4	0.22	1967.6
	0.05	-1.7	0.25	603.7
	0.1	1.9	0.4	348.9

5.2 Single UO_2 Assembly Problem

The second problem consists of a single UO_2 assembly, and the fuel rods are described with heterogeneity as shown in Fig. 5. Seven-group cross sections are sourced from the C5G7 benchmark problem [14], and the information pertaining to delayed neutron precursors is sourced from the literature [15]. All control rods are initially inserted 7.14 cm in the active core, and the perturbation is originated from all rod ejection in 0.1 sec. The reference calculation was carried out by the NLG iteration without the PCQS method with 0.5 ms, since this problem requires less than 1 ms time step size to obtain an accurate solution.

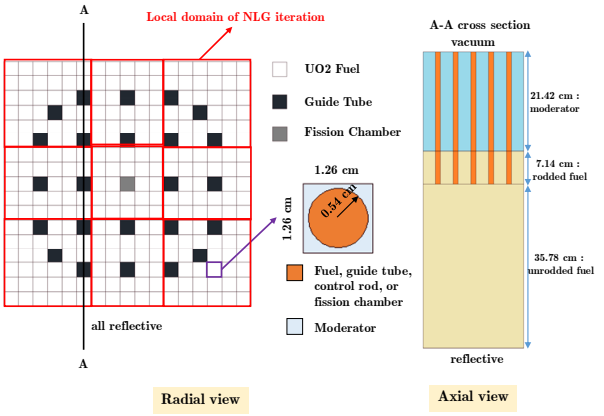

Fig. 5. Geometry (single UO_2 assembly)

The results are shown in Figs. 6, 7 and Table II. PCQS well predicts the reference solution with the relatively large time step size as shown in Figs 6 and 7. As shown in Table II, PCQS is still accurate with the 0.02 sec time step size, while DIRECT cannot use this order of time step size to provide the accurate solution. The computing time is reduced if a large time step size is used. If 4 % error is allowable, PCQS can use the 0.1 sec time step size, which is relatively a large time step size in the transport calculation (0.5 ms in this problem). With the same time step size, DIRECT takes less computing time than PCQS as shown in Table II, since PCQS takes more computing time to reflect accurate delayed neutron precursor densities after 0.1 sec. In other words, PCQS corrects the predicted flux, and this causes a longer computing time to find the solution which reflects the corrected flux from the previous time step. However, the faster computing in DIRECT is not meaningful due to the large errors in this problem.

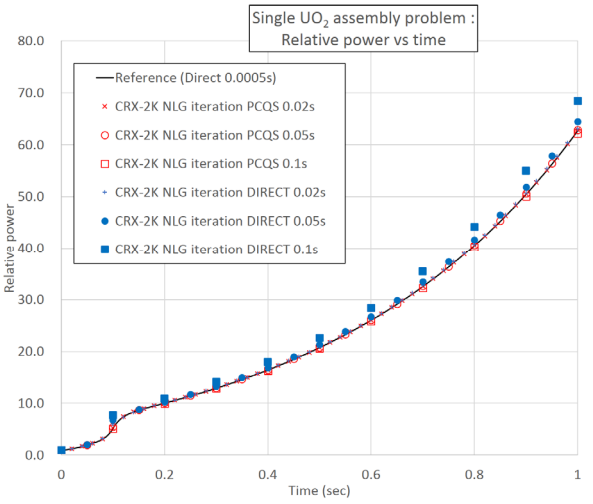

Fig. 6. Relative power vs time (single UO_2 assembly)

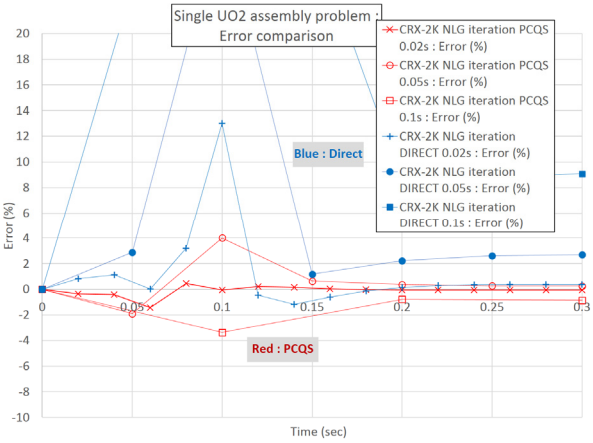

Fig. 7. Percentage error vs time (single UO_2 assembly)

Table II: Results summary (single UO_2 assembly)

Method	Time step size (sec)	Error (%) at 0.1 sec	Computing time (sec)
DIRECT	0.02	13.0	5690.2
	0.05	29.3	3161.3
	0.1	47.2	1927.7
PCQS	0.02	-0.1	12761.6
	0.05	4.0	5524.3
	0.1	-3.4	3107.9

6. Conclusions

The PCQS method is applied to the transient NLG iteration with the 2-D/1-D fusion transport kernel and the global p-CMFD wrapper, and has been implemented in CRX-2K. In the numerical problems, the PCQS method with the NLG iteration shows more accurate solutions compared to the direct transient calculations with large time step sizes.

However, the PCQS method may give an inaccurate solution if the shape function changes significantly in time, that follows from the basic assumption of the PCQS (or any kind of QS family) method. Therefore, a problem such as a MOX fuel-loaded problem, that would lead to a large change in shape function, is planned for future work.

References

[1] B. Cho and N. Z. Cho, "A Nonoverlapping local/global iterative method with 2-D/1-D fusion transport kernel and p-CMFD wrapper for transient reactor analysis," *Ann. Nucl. Energy* **85**, 937 (2015).

[2] B. Cho and N. Z. Cho, "Parallelization on nonoverlapping local/global iterative method with 2-D/1-D fusion transport kernel and p-CMFD wrapper for transient reactor analysis," Trans. Kor. Nucl. Soc., Gyeongju, Korea, October 29 – 30, 2015 (this meeting).

[3] J. Y. Cho et al., "Transient capability of the DeCART code," KAERI, KAERI/TR-2930 (2005).

[4] A. Zhu et al., "Transient methods for pin-resolved whole core transport using the 2D-1D methodology in MPACT," Joint International Conference on Mathematics and Computation (M&C 2015), Nashville, USA, April 19 – 23, 2015.

[5] S. Dulla, E. H. Mund, and P. Ravetto, "The quasi-static method revisited," *Prog. Nucl. Energy* **50**, 908 (2008).

[6] A. F. Henry, "Nuclear-Reactor Analysis," The MIT Press, 1975.

[7] N. Z. Cho, "The partial current-based CMFD (p-CMFD) method revisited," Trans. Kor. Nucl. Soc., Gyeongju, Korea, October 25 – 26, 2012 <http://www.kns.org/kns_files/kns/file/229%C1%B6%B3%B2%C1%F8.pdf>.

[8] N. Z. Cho, G. S. Lee, and C. J. Park, "Partial current-based CMFD acceleration of the 2D/1D fusion method for 3D whole-core transport calculations," *Trans. Am. Nucl. Soc.* **88**, 594 (2003).

[9] A. Zhu et al., "The implementation and analysis of the MOC and CMFD adjoint capabilities in the 2D-1D code MPACT," Joint International Conference on Mathematics and Computation (M&C 2015), Nashville, USA, April 19 – 23, 2015.

[10] A. F. Henry, "The application of reactor kinetics to the analysis of experiments," *Nucl. Sci. Eng.* **3**, 52 (1958).

[11] A. F. Henry and N. J. Curlee, "Verification of a method for treating neutron space–time problems," *Nucl. Sci. Eng.* **4**, 727 (1958).

[12] W. H. Reed and K. F. Hansen, "Alternating direction methods for the reactor kinetics equations," *Nucl. Sci. Eng.*, **41**, 431 (1970).

[13] L. A. Hageman and J. B. Yasinsky, "Comparison of alternating-direction time-differencing methods with other implicit methods for the solutions of the neutron group-diffusion equations," *Nucl. Sci. Eng.*, **38**, 8 (1969).

[14] M. A. Smith, E. E. Lewis, and B-C. Na, "Benchmark on deterministic transport calculations without spatial homogenization: A 2-D/3-D MOX fuel assembly 3-D benchmark," NEA/NSC/DOC(2003) 16. Organization for Economic Co-operation and Development, Nuclear Energy Agency (2003).

[15] V. F. Boyarinov, A. E. Kondrushin, and P. A. Fomichenko, "Benchmark on deterministic time-dependent transport calculations without spatial homogenisation," PHYSOR 2014, Kyoto, Japan, September 28 – October 3, 2014.